THE JOURNAL OF PHYSICAL CHEMISTRY Letters

pubs.acs.org/JPCL

Letter

Site-Specific Pressure-Driven Spin-Crossover in $Lu_{1-x}Sc_xFeO_3$

Ting Wen, Yiming Wang, Chen Li, Dequan Jiang, Zimin Jiang, Shangqing Qu, Wenge Yang,* and Yonggang Wang*

Cite This: *J. Phys. Chem. Lett.* 2020, 11, 8549–8553

Read Online

ACCESS | Metrics & More | Article Recommendations | Supporting Information

ABSTRACT: Pressure-driven spin-crossover (PSCO) is a collective quantum phenomenon frequently observed in transition-metal-based systems. According to the crystal-field theory, PSCO highly depends on the surrounding coordination environment of a given magnetic ion; nevertheless, it has never been verified experimentally up to now. Herein, we report the observation of a site-specific PSCO phenomenon in $Lu_{1-x}Sc_xFeO_3$, in which octahedrally coordinated Fe^{3+} in orthorhombic $LuFeO_3$ and trigonal-bipyramidally coordinated Fe^{3+} in hexagonal $Lu_{0.5}Sc_{0.5}FeO_3$ show distinct PSCO response to external pressure. X-ray emission spectra and DFT calculations reveal the key role of coordination environment in a PSCO process and predict the occurrence of PSCO for trigonal-bipyramidally coordinated Fe^{3+} above 100 GPa, far beyond that of 50 GPa for octahedrally coordinated Fe^{3+} in $LuFeO_3$. The demonstration of site-specific PSCO sheds light on the state-of-the-art design of PSCO materials for directional applications.

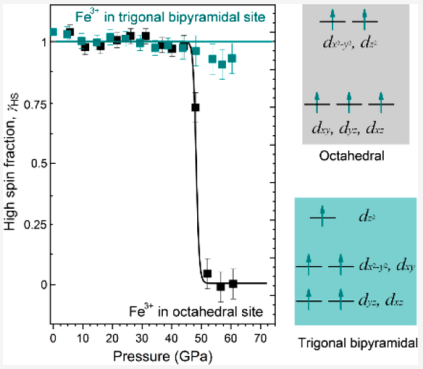

Spin-crossover (SCO), as a consequence of the d-orbital splitting in a ligand field, is generally characterized by transition-metal centers undergoing a spin state transition in response to external stimuli such as heat, light, pressure, and magnetic fields.[1−4] Typically, SCO is observed in first-row transition-metal complexes with electronic configurations d^4 to d^7. To date, the well-studied SCO system is $Fe^{2+}(d^6)$-based complexes with an FeL_6 coordination manner.[5,6] Because the molecular bistable status of SCO is associated with a lack of fatigue, SCO materials hold great promise for applications in sensors, displays, and digital memory. Particularly, when a classical light- or temperature-initiated SCO arises along with structural phase transitions and/or physical property alterations, SCO materials can become multifunctional.[7−10]

Although not as common as light- or temperature-initiated SCO, pressure-driven SCO (PSCO) has also been frequently reported in many material systems. Pressure, as an alternative external stimulus to light or temperature, is the most direct route to altering the crystal-field strength by shortening the metal−ligand distances and thus can drive SCO especially in strongly correlated systems.[11,12] That is, benefitting from the power of pressure, the exploration of PSCO material has no longer been limited to the soft metal−organic complex system. Surprisingly, to date, PSCO has been reported more as only a physical phenomenon[13−19] rather than a useful functionality for modern material design. We have focused on this issue for a long time and successfully developed a series of materials with abrupt PSCO following the principle to reduce the dimensionality of metal centers to increase the "cooperativity" between them.[20−22]

According to the crystal-field theory, the ground spin state of a metal center embedded in a crystalline matrix is determined by the relative magnitude of the d-orbital splitting energy (Δ) along with the Hund's intra-atomic exchange energy (J).[23,24] In weak fields ($\Delta < J$), the ground state is high spin (HS) with a maximum spin multiplicity, whereas strong fields ($\Delta > J$) stabilize the low spin (LS) state with a minimum multiplicity. For different d-orbital splitting situations, the effect of pressure on the compression deformation behavior of metal−ligand polyhedra and also the change of Δ is different. Therefore, PSCO should be highly dependent on the surrounding coordination environment of a given magnetic ion; nevertheless, this viewpoint has never been experimentally verified to date. In this work, we studied the site-specific PSCO phenomenon in $Lu_{1-x}Sc_xFeO_3$, which perfectly provides two distinct coordination environments for Fe^{3+} (octahedral at x = 0 and trigonal-bipyramidal at x = 0.5, respectively). *In situ* synchrotron X-ray diffraction (XRD) and X-ray emission spectroscopy (XES) experiments were performed to verify the PSCO behavior of Fe^{3+}. Density function theory (DFT) calculations were also conducted to reveal the spin state evolutions of Fe^{3+} in different crystal fields under high pressure.

Received: August 19, 2020
Accepted: September 17, 2020
Published: September 24, 2020

https://dx.doi.org/10.1021/acs.jpclett.0c02537
J. Phys. Chem. Lett. 2020, 11, 8549−8553

$Lu_{1-x}Sc_xFeO_3$ possesses a characteristic structure sequence of rare-earth orthoferrites along with the increase of Sc content.[25−30] $LuFeO_3$ and $Lu_{0.5}Sc_{0.5}FeO_3$ fine powders were synthesized via a sol−gel method followed by high-temperature sintering (for details, see the Supporting Information). XRD analyses prove their high phase purity and crystallinity in orthorhombic and hexagonal symmetry, respectively (Figure S1). The crystal structures of $LuFeO_3$ and $Lu_{0.5}Sc_{0.5}FeO_3$ are shown in Figure 1. $LuFeO_3$ adopts a distorted perovskite

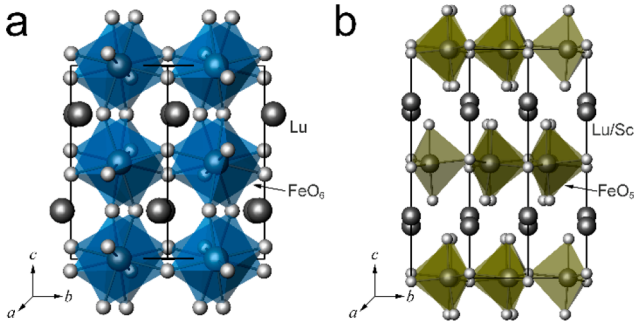

Figure 1. Crystal structures of (a) orthorhombic $LuFeO_3$ with octahedrally coordinated Fe^{3+} and (b) hexagonal $Lu_{0.5}Sc_{0.5}FeO_3$ with trigonal-bipyramidally coordinated Fe^{3+}.

structure in which all of the Fe^{3+} ions coordinate with six O^{2-} anions in an undistorted octahedral geometry. Comparatively, the hexagonal $Lu_{0.5}Sc_{0.5}FeO_3$ comprises closely packed layers of vertex-sharing FeO_5 bipyramids to form triangular lattices in the *ab* plane, which are separated by wrinkled Lu/Sc layers along the *c*-axis. All the Fe^{3+} ions are surrounded by three in-plane and two apical O^{2-} ligands. $LuFeO_3$ and $Lu_{0.5}Sc_{0.5}FeO_3$ provide a rare example of two analogues similar in composition but distinct in local structure, which enables the comparative study of site-specific PSCO.

In situ XES measurements on both samples loaded inside diamond anvil cells (DACs) were performed to probe the spin state evolution under high pressure and room temperature (for details, see the Supporting Information). Figure 2 presents the Fe Kβ XES spectra of $LuFeO_3$ and $Lu_{0.5}Sc_{0.5}FeO_3$ under compression up to 60 GPa, respectively. Typically, the XES spectra at low pressures comprise a main K$\beta_{1,3}$ peak located around 7058.6 eV and a satellite Kβ' peak located around 7044.6 eV. It is well-known that the Kβ lines are characteristic

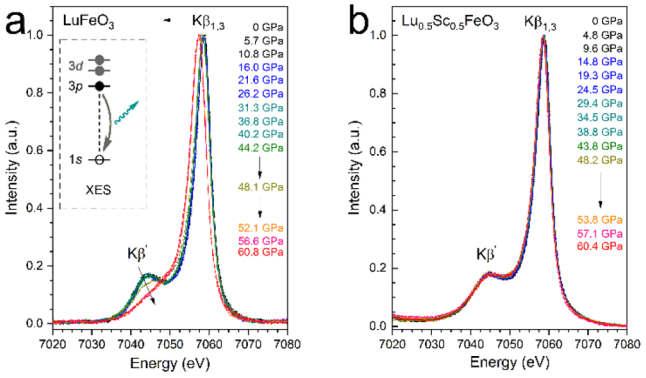

Figure 2. Fe K_β XES of (a) $LuFeO_3$ and (b) $Lu_{0.5}Sc_{0.5}FeO_3$ as a function of applied pressure. Inset of panel a shows the mechanism of an XES measurement to reflect the spin states of a 3d metal ion.

X-ray emissions originating from the 3p to 1s decay.[4] The parameters of Kβ lines, especially the intensity of Kβ' peaks, can reflect the interactions between the 3p core hole and the partially filled 3d shell electrons (inset of Figure 2). Therefore, the occurrence of an HS-to-LS transition can be distinguished simply by the decrease of Kβ' peaks and the left-shift of K$\beta_{1,3}$ peaks. For $LuFeO_3$, well-defined Kβ' satellite peaks are observed in the low-pressure range (below 44 GPa), indicating a HS ground state ($S = 5/2$). When pressure is greater than 48 GPa, the Fe Kβ' peak starts to decrease and becomes indistinguishable above 52 GPa, and the Fe K$\beta_{1,3}$ lines shift to lower energies correspondingly. This evidence indicates the complete occurrence of PSCO of Fe^{3+} ($S = 5/2$ to $S = 1/2$) in $LuFeO_3$ around 50 GPa. Whereas, for $Lu_{0.5}Sc_{0.5}FeO_3$, no decrease of the Fe Kβ' peak or shift of the Fe K$\beta_{1,3}$ peak is observed up to 60 GPa, indicating the HS state of Fe^{3+} ($S = 5/2$) in hexagonal $Lu_{0.5}Sc_{0.5}FeO_3$ can survive to a higher pressure than that in orthorhombic $LuFeO_3$. The absence of PSCO in $Lu_{0.5}Sc_{0.5}FeO_3$ reveals the key impact of coordination environment surrounding transition-metal ions on the onset of a PSCO incident.

Structure analyses based on *in situ* XRD patterns provide a mutual corroboration along with XES evidence on the occurrence of PSCO in $LuFeO_3$ and the absence of PSCO in $Lu_{0.5}Sc_{0.5}FeO_3$. $LuFeO_3$ suffers an iso-structural phase transition around 49 GPa as evidenced by the abrupt shifts of representative XRD peaks (110), (002), and (111) to higher 2θ angles, corresponding to collapses of the cell parameters and the cell volume (Figures S2 and S3). This is in accordance with many previous experiences that PSCO usually occurs along with a lattice collapse.[31] Although there is no symmetry change, octahedral tilts of FeO_6 are very possible in the iso-structural phase transition referring to previous studies.[32] $Lu_{0.5}Sc_{0.5}FeO_3$ also undergoes an iso-structural phase transition around 45 GPa accompanied by a volume collapse (Figures S4 and S5). However, this volume collapse is not induced by the moment collapse of Fe^{3+}, but instead a distortion of FeO_5 trigonal bipyramids with elongation of the apical Fe−O bonds along the *c*-axis.

Quantitative analyses of the XES data were conducted following the IAD procedure described by Vankó et al.,[33] by which the IAD value reflects a linear relationship with the average spin quantum number, *S*. Figure 3a shows the pressure dependence of the Fe^{3+} spin state in $LuFeO_3$ and

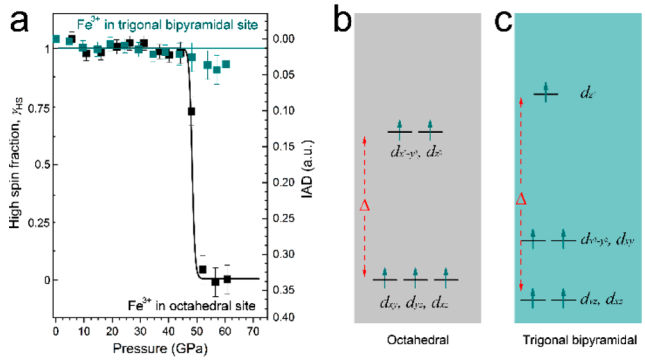

Figure 3. (a) Spin state fractions and IAD values derived from the Fe K_β XES spectra of $LuFeO_3$ and $Lu_{0.5}Sc_{0.5}FeO_3$ as a function of pressure. (b and c) Schematic diagrams of the d orbital splitting of Fe^{3+} in octahedrally and trigonal-bipyramidally coordinated environments, respectively.

https://dx.doi.org/10.1021/acs.jpclett.0c02537
J. Phys. Chem. Lett. 2020, 11, 8549−8553

$Lu_{0.5}Sc_{0.5}FeO_3$ from the IAD analysis. At low pressures, Fe^{3+} ions in both materials exhibit a high spin state with $S = 5/2$ (IAD ≈ 0). As the pressure approaches 50 GPa, the IAD value for $LuFeO_3$ increases abruptly indicating the occurrence of PSCO for Fe^{3+} in the octahedral sites. For $Lu_{0.5}Sc_{0.5}FeO_3$, the IAD value remains close to 0 and the high spin fraction remains nearly 100% up to more than 60 GPa. The site-specific PSCO in $LuFeO_3$ and $Lu_{0.5}Sc_{0.5}FeO_3$ can be explained by the crystal-field theory. It is well-known that the spin state of a transition-metal ion depends on the competition between the d-orbital splitting energy (Δ = 10 Dq) and the electronic Coulomb repulsion (J). In an octahedral coordination field for Fe^{3+} ions in $LuFeO_3$, the five d orbitals split into 3-fold degenerated d_{xy}, d_{yz}, and d_{xz} and 2-fold degenerated $d_{x^2-y^2}$ and d_{z^2} (Figure 3b). In this configuration, high-pressure drives the increase of Δ markedly and most iron(III) oxides with an octahedral coordination manner undergo PSCO between 35 and 50 GPa. In the rare trigonal bipyramidal coordination field for Fe^{3+} ions in hexagonal $Lu_{0.5}Sc_{0.5}FeO_3$, the five d orbitals split into two lower d_{xz} and d_{yz}, two intermediate d_{xy} and $d_{x^2-y^2}$, and a highest d_{z^2} (Figure 3c). Although Δ is always a little higher than that within an octahadral field, trigonal-bipyramidally coordinated Fe^{3+} ions still adopt HS state at ambient conditions. It is worth mentioning that, under high pressure, one electron may jump from d_{z^2} to the lowest d_{xz} or d_{yz}, which results in an intermediate spin (IS) state with $S = 3/2$ rather than a LS state with $S = 1/2$. During the LP-to-HP phase transition (very likely HS-to-IS), the elongation of the apical Fe−O bonds within FeO_5 trigonal bipyramids leads to lower d_{z^2} orbital and thus decrease Δ (Figure S6), which inhibits the occurrence of PSCO in hexagonal $Lu_{0.5}Sc_{0.5}FeO_3$. After that, high pressure will keep shortening all the Fe−O bonds (increasing Δ) and finally leads to the occurrence of PSCO (HS-to-IS) at a higher pressure. Moreover, we mention the possible impact of deviatoric stress, frequently observed in nanosystems,[34,35] on the occurrence of structural phase transition and PSCO in $Lu_{1-x}Sc_xFeO_3$. The use of silicone oil as the pressure-transmitting medium (PTM) may slightly affect the occurrence pressure of the iso-structural phase transitions and the steepness of PSCO in $Lu_{1-x}Sc_xFeO_3$, whereas the phenomenon of site-specific PSCO will not be changed by the PTM effect.

DFT calculations based on the HS, IS, and LS states of Fe^{3+} were performed to validate the role of coordination environments in the PSCO process of Fe^{3+} within $LuFeO_3$ and $Lu_{0.5}Sc_{0.5}FeO_3$. For simplicity and ease of comparison, two $LuFeO_3$ structures, one with an orthorhombic symmetry (ICSD# 27285)[36] and the other with the hexagonal $Lu_{0.5}Sc_{0.5}FeO_3$ structure were adopted for the DFT calculations (for details, see the Supporting Information). LDA+U method with U = 4.3 eV was adopted by comparing the experimental cell volumes with those from calculations (Figure S7). For orthorhombic $LuFeO_3$ with octahedrally coordinated Fe^{3+}, a pressure-driven HS-to-LS transition occurs around 60 GPa, meeting but a little higher than the experimental result (Figure 4a). For hexagonal $LuFeO_3$ with trigonal-bipyramidally coordinated Fe^{3+}, first, the HS state remains in the ground state up to 70 GPa within the experimentally verified pressure range. Linear extension predicts a PSCO point (HS-to-IS transition) of Fe^{3+} around 100 GPa, and finally to a LS state at very high pressure (more than 150 GPa) (Figure 4b). Both our experimental and calculation results reveal the site-specific feature of the PSCO phenomenon. It is expected that a transition-metal ion within different crystal field will exhibit distinct PSCO behaviors, whereas it is unexpected that there would be such a big difference between the two situations (60 GPa in octahedron versus 145 GPa in trigonal-bipyramid). Benefiting from the difference brought by crystal field strength, it is possible to design tailored PSCO materials for specific application scenarios.

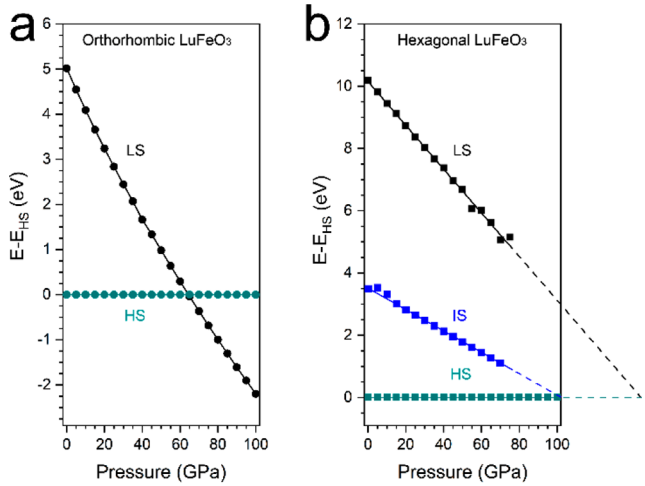

Figure 4. Relative total energy calculated for the HS, IS, and LS states in (a) orthorhombic $LuFeO_3$ with octahedrally coordinated Fe^{3+} and (b) hexagonal $LuFeO_3$ with trigonal-bipyramidally coordinated Fe^{3+}.

In summary, we report a site-specific PSCO phenomenon in the $Lu_{1-x}Sc_xFeO_3$ system for the first time. Besides the similar chemical composition, $LuFeO_3$ and $Lu_{0.5}Sc_{0.5}FeO_3$ have distinct coordination environments for Fe^{3+} ions: octahedrally coordinated in orthorhombic $LuFeO_3$ and trigonal-bipyramidally coordinated in hexagonal $Lu_{0.5}Sc_{0.5}FeO_3$. They show distinct PSCO as evidenced by both experimental results (XES and XRD) and theoretical calculations. Fe^{3+} within the octahedral FeO_6 sites undergoes a PSCO around 50 GPa ($S = 5/2$ to $S = 1/2$). Comparatively, no PSCO occurs experimentally up to 60 GPa for Fe^{3+} within the trigonal-bipyramidal FeO_5 sites, which is predicated to happen above 100 GPa. These results validate the key role of coordination environment in a PSCO process. The demonstration of site-specific PSCO paves the way to precise design of novel pressure-responsive switch materials for various practical applications.

EXPERIMENTAL METHODS

Sample Preparation. $LuFeO_3$ and $Lu_{0.5}Sc_{0.5}FeO_3$ powders were synthesized using a sol−gel method followed by high-temperature sintering. The phase purity was confirmed by powder XRD at room temperature and ambient pressure.

High-Pressure Experiments. A symmetrical diamond anvil cell (DAC) was employed to generate high pressure. A steel gasket was preindented to about 40 μm in thickness followed by laser-drilling the central part to form a 120 μm diameter hole to serve as the sample chamber. Precompressed $LuFeO_3$ and $Lu_{0.5}Sc_{0.5}FeO_3$ pellets and ruby ball were loaded in the chamber. Silicone oil was used as the pressure-transmitting medium. The *in situ* angle-dispersive X-ray diffraction (ADXRD) experiments were carried out at the BL15U1 beamline station of Shanghai Synchrotron Radiation Facility (SSRF) at room temperature. A focused monochromatic X-ray beam with wavelength of 0.6199 Å was used for the diffraction

https://dx.doi.org/10.1021/acs.jpclett.0c02537
J. Phys. Chem. Lett. 2020, 11, 8549−8553

experiments, and the ADXRD patterns were recorded by a MAR165 CCD detector. For the high-pressure X-ray emission spectrum (XES) experiments performed at 16 ID-D station of HPCAT, Be gaskets were used as the sample chamber and silicone oil was used as pressure-transmitting medium.

DFT Calculations. Two $LuFeO_3$ structures, one with an orthorhombic symmetry and the other with the hexagonal $Lu_{0.5}Sc_{0.5}FeO_3$ structure were adopted for the DFT calculations. DFT calculations were performed using the VASP package, and the electron−electron interaction is treated using the LDA+U with $U = 4.3$ eV; $J = 0$; energy cutoff, 600 eV; and k points, 6 × 6 × 4. The PAW−PBE pseudopotential is used, and valence electronics of Lu, Fe, and O are $5p^6 5d^1 6s^2$, $3d^7 4s^1$, and $2s^2 2p^4$, respectively.

■ ASSOCIATED CONTENT

Supporting Information

The Supporting Information is available free of charge at https://pubs.acs.org/doi/10.1021/acs.jpclett.0c02537.

Experimental details, characterization data, theoretical calculations, and supplemental figures (PDF)

■ AUTHOR INFORMATION

Corresponding Authors

Wenge Yang − *Center for High Pressure Science and Technology Advanced Research (HPSTAR), Beijing 100094, China*; Email: yangwg@hpstar.ac.cn

Yonggang Wang − *Center for High Pressure Science and Technology Advanced Research (HPSTAR), Beijing 100094, China*; orcid.org/0000-0003-4816-9182; Email: yonggang.wang@hpstar.ac.cn

Authors

Ting Wen − *Center for High Pressure Science and Technology Advanced Research (HPSTAR), Beijing 100094, China*; orcid.org/0000-0001-6572-0920

Yiming Wang − *Center for High Pressure Science and Technology Advanced Research (HPSTAR), Beijing 100094, China*

Chen Li − *Center for High Pressure Science and Technology Advanced Research (HPSTAR), Beijing 100094, China*

Dequan Jiang − *Center for High Pressure Science and Technology Advanced Research (HPSTAR), Beijing 100094, China*

Zimin Jiang − *Center for High Pressure Science and Technology Advanced Research (HPSTAR), Beijing 100094, China*

Shangqing Qu − *Center for High Pressure Science and Technology Advanced Research (HPSTAR), Beijing 100094, China*

Complete contact information is available at: https://pubs.acs.org/10.1021/acs.jpclett.0c02537

Notes

The authors declare no competing financial interest.

■ ACKNOWLEDGMENTS

This work was supported by National Key R&D Program of China (2018YFA0305900) and National Natural Science Foundation of China (Grant Nos. 51527801 and U1930401). High-pressure XRD data were collected at beamline station BL15U1 of Shanghai Synchrotron Radiation Facility (SSRF), Shanghai, China. High-pressure XES data were collected at 16-ID-D, APS, Argonne National Laboratory. HPCAT operations are supported by DOE-NNSA under Award No. DE-NA0001974 with partial instrumentation funding by NSF. APS is supported by DOE-BES, under contract No. DE-AC02-06CH11357.

■ REFERENCES

(1) Real, J. A.; Gaspar, A. B.; Muñoz, M. C. Thermal, pressure and light switchable spin-crossover materials. *Dalton Trans* **2005**, 2062−2079.

(2) Gütlich, P.; Garcia, Y.; Goodwin, H. A. Spin crossover phenomena in Fe (ii) complexes. *Chem. Soc. Rev.* **2000**, *29*, 419−427.

(3) Bousseksou, A.; Molnár, G.; Salmon, L.; Nicolazzi, W. Molecular spin crossover phenomenon: recent achievements and prospects. *Chem. Soc. Rev.* **2011**, *40*, 3313−3335.

(4) Gütlich, P.; Ksenofontov, V.; Gaspar, A. B. Pressure effect studies on spin crossover systems. *Coord. Chem. Rev.* **2005**, *249*, 1811−1829.

(5) Weber, B.; Bauer, W.; Obel, J. An iron (II) spin-crossover complex with a 70 K wide thermal hysteresis loop. *Angew. Chem., Int. Ed.* **2008**, *47*, 10098−10101.

(6) König, E.; Ritter, G.; Kulshreshtha, S. K. The nature of spin-state transitions in solid complexes of iron (II) and the interpretation of some associated phenomena. *Chem. Rev.* **1985**, *85*, 219−234.

(7) Ohkoshi, S.; Imoto, K.; Tsunobuchi, Y.; Takano, S.; Tokoro, H. Light-induced spin-crossover magnet. *Nat. Chem.* **2011**, *3*, 564−569.

(8) Boldog, I.; Gaspar, A. B.; Martínez, V.; Pardo-Ibañez, P.; Ksenofontov, V.; Bhattacharjee, A.; Gütlich, P.; Real, J. A. Spin-crossover nanocrystals with magnetic, optical, and structural bistability near room temperature. *Angew. Chem., Int. Ed.* **2008**, *47*, 6433−6437.

(9) Larionova, J.; Salmon, L.; Guari, Y.; Tokarev, A.; Molvinger, K.; Molnár, G.; Bousseksou, A. Towards the ultimate size limit of the memory effect in spin-crossover solids. *Angew. Chem., Int. Ed.* **2008**, *47*, 8236−8240.

(10) Gaspar, A. B.; Ksenofontov, V.; Seredyuk, M.; Gütlich, P. Multifunctionality in spin crossover materials. *Coord. Chem. Rev.* **2005**, *249*, 2661−2676.

(11) Kuneš, J.; Lukoyanov, A. V.; Anisimov, V. I.; Scalettar, R. T.; Pickett, W. E. Collapse of magnetic moment drives the Mott transition in MnO. *Nat. Mater.* **2008**, *7*, 198−202.

(12) Rueff, J.-P.; Kao, C.-C.; Struzhkin, V. V.; Badro, J.; Shu, J.; Hemley, R. J.; Mao, H. K. Pressure-induced high-spin to low-spin transition in FeS evidenced by X-ray emission spectroscopy. *Phys. Rev. Lett.* **1999**, *82* (16), 3284−3287.

(13) Kantor, I. Y.; Dubrovinsky, L. S.; McCammon, C. A. Spin crossover in (Mg,Fe)O: A Mössbauer effect study with an alternative interpretation of x-ray emission spectroscopy data. *Phys. Rev. B: Condens. Matter Mater. Phys.* **2006**, *73*, No. 100101.

(14) Badro, J.; Struzhkin, V. V.; Shu, J.; Hemley, R. J.; Mao, H.-K.; et al. Magnetism in FeO at megabar pressures from X-ray emission spectroscopy. *Phys. Rev. Lett.* **1999**, *83*, 4101−4104.

(15) Lin, J.-F.; Struzhkin, V. V.; Jacobsen, S. D.; Hu, M. Y.; Chow, P.; Kung, J.; Liu, H.; Mao, H.-K.; Hemley, R. J. Spin transition of iron in magnesiowüstite in the Earth's lower mantle. *Nature* **2005**, *436*, 377−380.

(16) Li, J.; Struzhkin, V. V.; Mao, H.-K.; Shu, J.; Hemley, R. J.; Fei, Y.; Mysen, B.; Dera, P.; Prakapenka, V.; Shen, G. Electronic spin state of iron in lower mantle perovskite. *Proc. Natl. Acad. Sci. U. S. A.* **2004**, *101*, 14027−14030.

(17) Ding, Y.; Haskel, D.; Ovchinnikov, S. G.; Tseng, Y.-C.; Orlov, Y. S.; Lang, J. C.; Mao, H.-K. Novel Pressure-Induced Magnetic Transition in Magnetite (Fe_3O_4). *Phys. Rev. Lett.* **2008**, *100*, 045508.

(18) Rosner, H.; Koudela, D.; Schwarz, U.; Handstein, A.; Hanfland, M.; Opahle, I.; Koepernik, K.; Kuz'min, M. D.; Müller, K.-H.; Mydosh, J. A.; Richter, M. Magneto-elastic lattice collapse in YCo_5. *Nat. Phys.* **2006**, *2*, 469−472.

(19) Gleason, A. E.; Quiroga, C. E.; Suzuki, A.; Pentcheva, R.; Mao, W. L. Symmetrization driven spin transition in ϵ-FeOOH at high pressure. *Earth Planet. Sci. Lett.* **2013**, *379*, 49−55.
(20) Wang, Y.; Zhou, Z.; Wen, T.; Zhou, Y.; Li, N.; Han, F.; Xiao, Y.; Chow, P.; Sun, J.; Pravica, M.; Cornelius, A. L.; Yang, W.; Zhao, Y. Pressure-driven cooperative spin-crossover, large-volume collapse, and semiconductor-to-metal transition in manganese (II) honeycomb lattices. *J. Am. Chem. Soc.* **2016**, *138*, 15751−15757.
(21) Wang, Y.; Ying, J.; Zhou, Z.; Sun, J.; Wen, T.; Zhou, Y.; Li, N.; Zhang, Q.; Han, F.; Xiao, Y.; Chow, P.; Yang, W.; Struzhkin, V. V.; Zhao, Y.; Mao, H.-k. Emergent superconductivity in an iron-based honeycomb lattice initiated by pressure-driven spin-crossover. *Nat. Commun.* **2018**, *9*, 1914.
(22) Wen, T.; Wang, Y.; Li, N.; Zhang, Q.; Zhao, Y.; Yang, W.; Zhao, Y.; Mao, H.-k. Pressure-Driven Reversible Switching between n- and p-Type Conduction in Chalcopyrite $CuFeS_2$. *J. Am. Chem. Soc.* **2019**, *141*, 505−510.
(23) Lyubutin, I. S.; Ovchinnikov, S. G.; Gavriliuk, A. G.; Struzhkin, V. V. Spin-crossover-induced Mott transition and the other scenarios of metallization in $3d^n$ metal compounds. *Phys. Rev. B: Condens. Matter Mater. Phys.* **2009**, *79*, 085125.
(24) Wentzcovitch, R. M.; Justo, J. F.; Wu, Z.; da Silva, C. R. S.; Yuen, D. A.; Kohlstedt, D. Anomalous compressibility of ferropericlase throughout the iron spin crossover. *Proc. Natl. Acad. Sci. U. S. A.* **2009**, *106*, 8447−8452.
(25) Masuno, A.; Ishimoto, A.; Moriyoshi, C.; Hayashi, N.; Kawaji, H.; Kuroiwa, Y.; Inoue, H. Weak Ferromagnetic Transition with a Dielectric Anomaly in Hexagonal $Lu_{0.5}Sc_{0.5}FeO_3$. *Inorg. Chem.* **2013**, *52*, 11889−11894.
(26) Masuno, A.; Ishimoto, A.; Moriyoshi, C.; Kawaji, H.; Kuroiwa, Y.; Inoue, H. Expansion of the Hexagonal Phase-Forming Region of $Lu_{1-x}Sc_xFeO_3$ by Containerless Processing. *Inorg. Chem.* **2015**, *54*, 9432−9437.
(27) Adams, D. J.; Amadon, B. Study of the volume and spin collapse in orthoferrite $LuFeO_3$ using LDA+U. *Phys. Rev. B: Condens. Matter Mater. Phys.* **2009**, *79*, 115114.
(28) Liu, F.; Xu, C.; Shen, S.; Li, N.; Guo, H.; Lü, X.; Xiang, H.; Bellaiche, L.; Zhao, J.; Yin, L.; Yang, W.; Wang, W.; Shen, J. Pressure-induced large enhancement of Néel temperature and electric polarization in the hexagonal multiferroic $Lu_{0.5}Sc_{0.5}FeO_3$. *Phys. Rev. B: Condens. Matter Mater. Phys.* **2019**, *100*, 214408.
(29) Lin, L.; Zhang, H. M.; Liu, M. F.; Shen, S.; Zhou, S.; Li, D.; Wang, X.; Yan, Z. B.; Zhang, Z. D.; Zhao, J.; Dong, S.; Liu, J.-M. Hexagonal phase stabilization and magnetic orders of multiferroic $Lu_{1-x}Sc_xFeO_3$. *Phys. Rev. B: Condens. Matter Mater. Phys.* **2016**, *93*, 075146.
(30) Leiner, J. C.; Kim, T.; Park, K.; Oh, J.; Perring, T. G.; Walker, H. C.; Xu, X.; Wang, Y.; Cheong, S.-W.; Park, J.-G. Magnetic excitations in the bulk multiferroic two-dimensional triangular lattice antiferromagnet (Lu,Sc)FeO_3. *Phys. Rev. B: Condens. Matter Mater. Phys.* **2018**, *98*, 134412.
(31) Rozenberg, G. KH.; Pasternak, M. P.; Xu, W. M.; Dubrovinsky, L. S.; Carlson, S.; Taylor, R. D. Consequences of pressure-instigated spin crossover in $RFeO_3$ perovskites: a volume collapse with no symmetry modification. *Europhys. Lett.* **2005**, *71* (2), 228−234.
(32) Vilarinho, R.; Bouvier, P.; Guennou, M.; Peral, I.; Weber, M. C.; Tavares, P.; Mihalik, M., Jr.; Mihalik, M.; Garbarino, G.; Mezouar, M.; Kreisel, J.; Almeida, A.; Moreira, J. A. Crossover in the pressure evolution of elementary distortions in $RFeO_3$ perovskites and its impact on their phase transition. *Phys. Rev. B: Condens. Matter Mater. Phys.* **2019**, *99*, 064109.
(33) Vankó, G.; Neisius, T.; Molnár, G.; Renz, F.; Kárpáti, S.; Shukla, A.; de Groot, F. M. F. Probing the 3d spin momentum with X-ray emission spectroscopy: The case of molecular-spin transitions. *J. Phys. Chem. B* **2006**, *110*, 11647−11653.
(34) Wang, Z.; Schliehe, C.; Wang, T.; Nagaoka, Y.; Cao, Y. C.; Bassett, W. A.; Wu, H.; Fan, H.; Weller, H. Deviatoric stress driven formation of large single-crystal PbS nanosheet from nanoparticles and in situ monitoring of oriented attachment. *J. Am. Chem. Soc.* **2011**, *133*, 14484−14487.
(35) Zhu, J.; Quan, Z.; Wang, C.; Wen, X.; Jiang, Y.; Fang, J.; Wang, Z.; Zhao, Y.; Xu, H. Structural evolution and mechanical behaviour of Pt nanoparticle superlattices at high pressure. *Nanoscale* **2016**, *8*, 5214−5218.
(36) Marezio, M.; Remeika, J. P.; Dernier, P. D. The crystal chemistry of the rare earth orthoferrites. *Acta Crystallogr., Sect. B: Struct. Crystallogr. Cryst. Chem.* **1970**, *26*, 2008−2022.

https://dx.doi.org/10.1021/acs.jpclett.0c02537
J. Phys. Chem. Lett. 2020, 11, 8549−8553